Biophysical Journal Volume 109 August 2015 461–468

Biophysical Perspective

Molecular Simulations of Gram-Negative Bacterial Membranes: A Vignette of Some Recent Successes

Jamie Parkin,[1] Matthieu Chavent,[2] and Syma Khalid[1,*]

[1]School of Chemistry, University of Southampton, Southampton, UK; and [2]Department of Biochemistry, University of Oxford, Oxford, UK

ABSTRACT In the following review we use recent examples from the literature to discuss progress in the area of atomistic and coarse-grained molecular dynamics simulations of selected bacterial membranes and proteins, with a particular focus on Gram-negative bacteria. As structural biology continues to provide increasingly high-resolution data on the proteins that reside within these membranes, simulations have an important role to play in linking these data with the dynamical behavior and function of these proteins. In particular, in the last few years there has been significant progress in addressing the issue of biochemical complexity of bacterial membranes such that the heterogeneity of the lipid and protein components of these membranes are now being incorporated into molecular-level models. Thus, in future we can look forward to complementary data from structural biology and molecular simulations combining to provide key details of structure-dynamics-function relationships in bacterial membranes.

The interaction of bacteria with their surrounding environment is mediated, directly or indirectly, through the membranes that constitute their cell envelopes. While bacteria are simple organisms, the cell envelopes that surround them are remarkably complex structures. The main distinguishing difference between Gram-negative and Gram-positive bacteria is that the cell envelope of the former has a double-membrane arrangement, in contrast to the single membrane of the latter. In both cases, the membranes provide a formidable barrier to permeation of solutes into and escape from, the cell. The outer membranes of Gram-negative bacteria are asymmetric in nature; the outer leaflet is composed almost exclusively of LPS (lipopolysaccharide) molecules, while the inner leaflet is composed of a mixture of ~25 different phospholipid types (when all of the different headgroup and tail combinations are included) (1) (Fig. 1). In contrast, the inner membrane is symmetric, containing only phospholipids in both leaflets, with a similar composition to the inner leaflet of the outer membrane. The single-cell membranes that protect Gram-positive bacteria are symmetric, although they often contain lipids that are more chemically complex than the phospholipids of Gram-negative bacteria, such as the lysyl-PG (lysyl-phosphatidylglycerol) lipids present in the *Staphylococcus aureus* membrane (2). Furthermore, the proteins that reside within the two membranes are also rather different in terms of their architectures. Based on known structures to date, inner membrane proteins generally tend to be composed of a number of *trans*-membrane helices, whereas outer membrane proteins almost invariably have a β-barrel architecture. A comprehensive list of known structures of membrane proteins is available at http://blanco.biomol.uci.edu/mpstruc/. Of the 1635 structures listed at the time of writing this review, ~600 were of bacterial membrane proteins. This relative paucity of structural data arises from inherent difficulties of working with membrane proteins due largely to their partially hydrophobic surfaces, flexibility, and lack of stability. Thus, even when structures are available they can often be of fairly low resolution, and can differ depending upon the method of structure determination. For example, the structures of the *Escherichia coli* outer-membrane proteins; OmpA, OmpX, and PagP, have been determined by both x-ray crystallography and nuclear magnetic resonance. The simulations revealed differences and similarities in the conformational dynamics of the proteins, although it was difficult to rationalize how much of the differences were due to the method of structure determination and how much to the variable resolution of the structures. Importantly, these and other similar studies reported in the literature have shown that, given long enough simulation times and structures of similar resolution, molecular dynamics (MD) is able to provide the link between membrane protein structures determined by different methods (3,4).

This chemical complexity in the composition of the membranes (5) presents something of a challenge for MD simulations, which have traditionally treated all types of bacterial membranes as homogeneous bilayers composed of a single phospholipid type (5). The simplification of these membranes has largely been due to 1) simplicity of simulation setup and 2) lack of parameters for complex lipids. Yet, there is compelling evidence from experimental and computational studies to indicate that the conformational dynamics of membrane proteins is tightly coupled to the behavior of the local lipid environment (6–8). A particularly limiting

Submitted February 18, 2015, and accepted for publication June 24, 2015.

*Correspondence: s.khalid@soton.ac.uk

Editor: Brian Salzberg.

0006-3495/15/08/0461/8

http://dx.doi.org/10.1016/j.bpj.2015.06.050

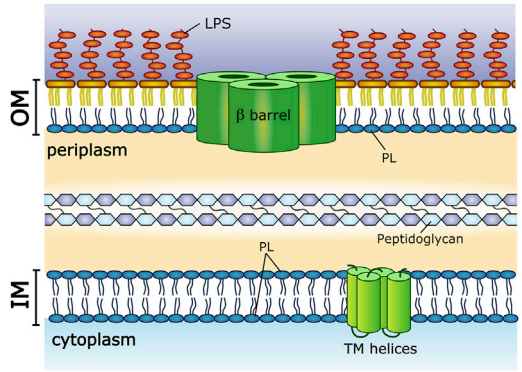

FIGURE 1 Schematic illustration of the cell envelope architecture of Gram-negative bacteria. To see this figure in color, go online.

factor at the atomistic level is the timescales accessible to such simulations; typically only hundreds of nanoseconds—not long enough, for example, to study the rearrangement of large extracellular loops or the encounter between a membrane protein and a ligand under equilibrium conditions.

These limitations have to some extent, been addressed by advances in computer hardware, enhanced sampling computational methodology, and the advent of coarse-grained models. Computer hardware enhancements have included more powerful supercomputers (an updated list of the top-500 supercomputers can be found at: http://www.top500.org), the exploitation of graphics processor unit technology by MD codes (9), and custom-built hardware designed specifically for MD simulations, such as the ANTON supercomputer built by D. E. Shaw Research (New York, NY) (10). An ANTON machine consists of application-specific integrated circuits, interconnected by a specialized high-speed, three-dimensional torus network. Crucially, for biological systems it has enabled atomistic simulations on the millisecond timescale, thus enabling testing and refinement of force fields that pave the way for longer, more accurate simulations (11). ANTON was recently employed to simulate the bacterial membrane protein BamA (12). Coarse-grained methods provide a route to accessing longer timescales through reducing the number of interaction sites of the models. Thus, the details of the individual atoms are sacrificed for the ability to simulate larger systems on longer timescales using similar resources to those for much slower atomistic simulations. For biological molecules, a number of models exist for proteins, lipids, carbohydrates, and nucleic acids; we refer the reader to the excellent text edited by G. A. Voth for details for coarse-grained models and methods (13).

In the following, we review progress in atomistic and coarse-grained MD simulations of bacterial membranes in the last 10 years by focusing on specific proteins from Gram-negative bacteria. As case studies we use largely, but not exclusively, examples from our own work and focus on conformational behavior of proteins already embedded within membranes and some more recent large-scale simulations that address protein-protein interactions within membrane models. Our discussion omits details of chemosensing and insertion of membrane proteins, which have both been the focus of a number of simulation studies, but we are unable to do justice to them here due to space limitations. Our aim is to show how understanding of the structure-function relationships of these proteins has grown via simulation studies, rather than to provide an exhaustive review of MD simulations of all bacterial membrane proteins over the last decade.

Protein-free membrane simulations

One of the most exciting developments in MD simulations of bacterial membranes in recent years has been the emergence of models that incorporate the heterogeneity of the nonprotein components. For example, a recent study reported atomistic simulations of a bacterial membrane mimetic composed of POPE (palmitoyloleoylglycerophosphatidylethanolamine) and POPG (palmitoyloleoylglycerophosphatidylglycerol) lipids in a 3:1 ratio (14). The simulations showed the impact of salt concentration on lipid mixing and water penetration into the bilayers, and demonstrated that microsecond timescales are adequate for mixing of these lipids. Atomistic models of LPS have been reported for each of the three most widely used families of force fields; CHARMM (www.charmm.org), AMBER (http://ambermd.org/), and GROMOS (www.gromos.net). In 2001, Lins and Straatsma (15) reported an LPS model composed of lipid A and core region from *Pseudomonas aeruginosa* parameterized using the AMBER95 (16) and GLYCAM_93 (17) force fields. Piggot et al. (18) reported an *E. coli* LPS model (lipid A and R1 core type), incorporated in a complex membranous environment, and modeled using the GROMOS53A6 force field (19). The *E. coli* model of Wu et al. (20) was parameterized using the CHARMM36 lipid and carbohydrate force fields (21–26), encompassing the lipid A, R1 core, and O6 antigen regions of the LPS in a symmetric bilayer.

The process of electroporation is often employed to provide a route for large drug molecules to cross biological membranes in vitro. The molecular rearrangements that occur during electroporation in phospholipid bilayers have previously been studied via MD simulation (27,28). Piggot et al. (18) recently reported comparative simulations of the pore-forming process in a Gram-positive (*S. aureus*) and Gram-negative (*E. coli*) bacterium. The results showed two distinct mechanisms of electroporation. Briefly, in the symmetric membrane of *S. aureus*, composed of PG (phosphatidylglycerol) lipids, lysyl-PG lipids, and diphosphatidylglycerol lipids (cardiolipin), the mechanism proceeds as follows: initially between three and five lipid headgroups move slightly toward the hydrophobic core of the bilayer. This is followed by water permeation into the core through the resulting defect in the headgroup region of the bilayer.

The molecules of water quickly extend through the bilayer core region and into the headgroups of the opposing leaflet, producing a continuous channel of water, which remains intact even when the magnitude of the applied electric field is drastically reduced.

In contrast, in the *E. coli* outer membrane (composed of LPS in the outer leaflet and a mixture of PE (phosphatidylethanolamine), PG, and cardiolipin in the inner leaflet), the water channel was only able to form once a phospholipid had flip-flopped from the inner leaflet into the outer. Upon reduction of the applied electric field, the water was observed to exit the bilayer core, after which the headgroup region resealed itself, giving a defect-free bilayer. These results show that individual LPS molecules in the outer leaflet are largely immobile because of tight cross-linking by cations and extended LPS-LPS hydrogen-bonding networks. Conversely, the phospholipid molecules in the inner leaflet diffuse much faster, enabling them to expel water and rapidly reseal the membrane, if defects do form. These structural and dynamic differences are likely to impact upon the mechanisms via which antimicrobials interact with the two membranes.

Bacterial inner membrane proteins

Bacterial inner membranes have a range of functions, including enzymatic activity, passive diffusion of ions, and active transport of solutes. Multidrug transporters or efflux proteins are membrane proteins that extrude antibiotics and other toxic compounds from within bacterial cells to the external milieu. A number of families of efflux proteins exist in bacteria; they are all thought to play a role in the development of resistant to antibiotics. As exemplars of efflux, here we focus on simulations of the multidrug and toxic compound extrusion (MATE) and resistance nodulation division (RND) families of multidrug transporters.

MATE transporters: NorM

Members of the MATE family of multidrug transporters use the difference in the electrochemical potential of H^+ or Na^+ ions across the membrane to drive drug transport. While full mechanistic details of solute extrusion are still unknown, the consensus view is of an overall mechanism in which the protein in its inward-facing conformation captures the solute from the interior of the cell, and then the protein adopts the outward facing conformation followed by entry of monovalent ions or protons, which bind within the protein. The small conformational changes that accompany movement of the ion lead to extrusion of the drug into the extracellular environment.

To date, three independent MD simulations studies of MATE transporters have been reported (29–31). Key details regarding the mechanism of action of the NorM MATE transporter from *Vibrio cholera* were reported from atomistic MD simulations by Vanni et al. (30), in which two Na^+ binding modes were observed. In the first binding mode, competitive binding between two acidic residues (E255 and D371) is established, with the ion binding alternatively to only one of the two residues, and in the second binding mode, the Na^+ is simultaneously bound to both of these residues. The second binding mode, in particular, shows the utility of molecular simulation, as it is unlikely to have been predicted from structural data, given the separation of E255 and D371, in the x-ray structure. Comparable simulations of this protein were also reported by Song et al. (29) in which the protein was simulated with and without Cs^+/Na^+ ions. The authors suggested that binding of two Na^+ ions simultaneously to the protein may be a requirement for the conformational transition to the inward-facing state of the protein. Leung et al. (31) performed atomistic MD simulations of the NorM MATE transporter from *Neisseria gonorrhea*. The drug-bound, outward-facing state of the protein was simulated, showing that cations can enter the central cavity of the protein from the periplasmic side, while the drug is already bound (Fig. 2). A possible two Na^+ ion-binding mode for the protein was also observed in the simulations. Interestingly, all three simulation studies of NorM revealed that the large extracellular vestibules of both proteins, suggested by the crystallographic data undergo partial collapse in a membrane environment. In the NorM transporter from *V. cholera*, Vanni et al. (30) showed

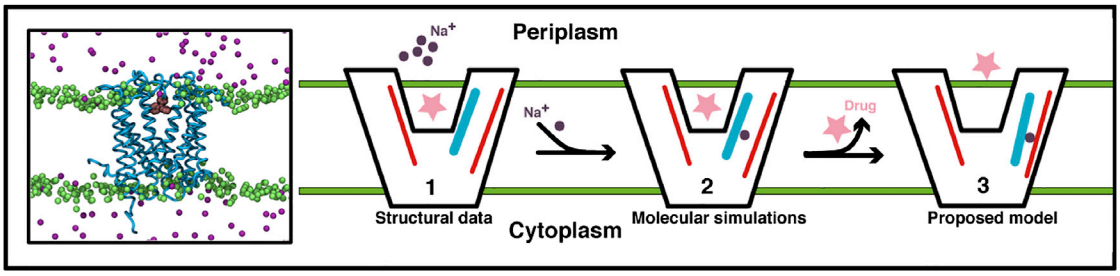

FIGURE 2 The NorM MATE transporter from *N. gonorrhea*. (*Left panel*) Snapshot extracted from the simulations of Leung et al. (31), in which the drug-bound x-ray structure (backbone representation of protein, spacefilling representation of the drug) is shown embedded within a POPC lipid bilayer (*green*), and surrounded by Na^+ ions (*spheres*). Lipid tails, water, and neutralizing anions have been removed for clarity. (*Right panel*) Schematic illustration of the proposed mechanism of drug extrusion. To see this figure in color, go online.

that the partial collapse of the vestibule led to formation of a twisting permeation pathway connecting the external environment with the catalytic site. The simulations have thus provided a testable hypothesis.

Resistance nodulation division pumps: acriflavine resistance protein B

The best-studied examples of resistance nodulation division (RND) pumps from the structural, biophysical, and simulation perspectives are the AcrAB-TolC complex in *E. coli* (32,33) and the MexAB-OprM complex in *P. aeruginosa* (34,35), where the inner membrane components are the homotrimeric proteins, acriflavine resistance protein B (AcrB), and MexB, respectively. Both inner membrane proteins utilize proton-motive force to expel a broad range of compounds out of the cell. A number of simulation studies of both the AcrB and MexB have been reported in the literature in recent years, but we refer the reader to the review by Fischer et al. (36) for a summary of these studies. The authors of the review have themselves contributed significantly to the understanding of RND pumps. For example, they studied hydration patterns via atomistic MD simulations to predict proton transfer pathways in AcrB; notably, these studies provided hypotheses directly testable by experimental approaches (37). The conformational rearrangements of AcrB that are associated with drug extrusion have also been studied by MD simulation. Schulz et al. (38) tested a number of hypotheses relating the structure through dynamics to the function of the protein. Their results enabled prediction of the pathway taken by the solute, once conformational changes have been induced. Thus, simulations have played major roles in understanding the mechanisms of action of RND transporters.

Bacterial outer membrane proteins

Conformational dynamics of outer membrane transporters in LPS-containing membrane models have also recently been reported (39,40). For example, simulations of the FecA transporter from *E. coli* allowed identification of specific interactions of the extracellular loops of the protein with the local environment. Comparative simulations of the same protein in a simple phospholipid bilayer showed that the LPS interactions are essential for the stability of key secondary structural elements within the protein. Similar LPS-protein interactions were also identified from simulations of the outer membrane enzyme, OmpLA (8).

Solutes are also able to enter and exit the outer membranes of Gram-negative bacteria through general porins and/or substrate-specific channels. For example, small solutes cross the outer membrane of *P. aeruginosa* through solute-specific channels such as the OprD and OpdK family of proteins (41,42). In contrast, permeation of small molecules through the outer membrane of *E. coli* occurs via large, nonspecific porins such as OmpC and OmpF (43,44). The molecular origins of the substrate permeation through these proteins have been the topic of a number of recent MD simulations, not least because these channels also represent major targets for antibiotics (45,46).

OprP

The outer membrane protein OprP from *P. aeruginosa* forms a phosphate-selective pore. The x-ray structure reveals the OprP monomer to be formed of a 16-stranded β-barrel with three loops, abundant in positively charged residues, folded into the lumen of the barrel (47). Arginine and lysine side chains located in these loops form a ladder-type structure along the pore axis, which includes the phosphate-binding site of OprP.

Pongprayoon et al. (48) reported an equilibrium and nonequilibrium atomistic MD investigation of the mechanism of phosphate permeation and selectivity in OprP. Notably, the potential-of-mean-force profile of phosphate permeation was calculated from umbrella sampling simulations. The potential-of-mean-force curves revealed the presence of two well-defined energy wells along the permeation pathway of inorganic phosphate (Pi) anion through the OprP pore. One of these energy wells corresponds to the Pi binding site revealed in the x-ray structure of OprP. The transition of the anion from this binding site to the one represented by the other energy well is facilitated by interaction with the side chain of residue K121. Encouragingly, structural and mutational studies had already proposed the mechanism of phosphate permeation to involve residue K121 (47,49). Residue R60 is involved in interactions with the Pi in both binding sites (Fig. 3). A dissociation constant of 6 μM was obtained from the standard free energy of phosphate binding to OprP. The authors noted that this high specificity is necessary for the biological function of OprP, which is to scavenge Pi ions under conditions of phosphate starvation.

The understanding of ion binding in OprP was further improved as Modi et al. (50,51) investigated the role of

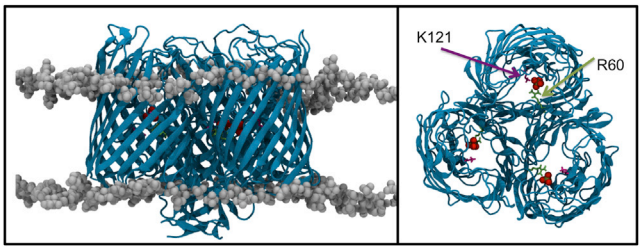

FIGURE 3 (*Left panel*) OprP embedded in a phospholipid bilayer. The protein backbone and lipid headgroups are shown explicitly. Water molecules have been removed for clarity. (*Right panel*) OprP simulation system viewed along the principal axis of the protein from the extracellular side. The phosphate group is located in the position corresponding to a binding site identified in the simulations of Pongprayoon et al. (48), where it is stabilized through interactions with residues including R60 and K121. To see this figure in color, go online.

two other charged residues. Specifically, the roles of residues D94 and R133 were explored via a combination of simulations and experiments. While, intuitively, the location of D94, an acidic residue, within the phosphate-binding site may seem puzzling, free-energy calculations revealed that D94 is essential for maintaining an appropriate phosphate-binding affinity within the channel. Electrostatic repulsion enables decreased phosphate residence time, thus preventing excessively strong binding of phosphate that would hinder permeation through the channel. Thus, the simulations have provided an energetic rationale for the importance of D94.

OprD

The outer membrane protein OprD/OccD1, from *P. aeruginosa*, is a porin selective for a single arginine monomer. X-ray structures revealed that OprD is an 18-stranded β-barrel with a series of arginine residues lining the lumen, forming a ladder that is associated with transport of the arginine substrate (52). The most favorable binding position during permeation of arginine through OprD was located near residues Y176, Y282, and D307 (53), which was predicted by docking calculations and MD simulations. Furthermore, it had been hypothesized that the OprD channel is likely to be rather flexible, in order to allow passage of solutes; this was subsequently proven by MD simulations.

Parkin and Khalid (54) used steered MD simulations to predict that the pathway of arginine through the channel of OprD can be described as a three-stage process: initial positioning of arginine in the opening of the pore, followed by reorientation of arginine for passage through the eyelet region of the protein (narrowest constriction), and finally ejection of arginine from the protein. Once in the eyelet region, for successful transport arginine is required to adopt an orientation in which the backbone carboxylate group is closer to the periplasmic space than the side-chain guanidinium group (see Fig. 4). This orientation allows a series of hydrogen-bonding and electrostatic interactions with residues in the extracellular loops and electrostatic interactions with arginine residues that are part of the ladder. The simulations showed that the carboxylate group of the arginine follows a defined pathway through the protein, roughly following the pathway of the arginine ladder.

Simulations of the general porins of *E. coli*, in particular OmpC and OmpF, have been the focus of many simulation studies over the years. For example, Kumar et al. (55) and Singh et al. (56) reported studies of the permeation of the antibiotics ampicillin and enrofloxacin through OmpF using equilibrium MD and metadynamics simulations, and permeation of norfloxacin through OmpF and OmpC was considered in a comparative study (57). Due to space limitations, a thorough consideration of this topic is not possible here, but we refer the reader to some recent reviews of computational studies of these and other membrane proteins (58–61).

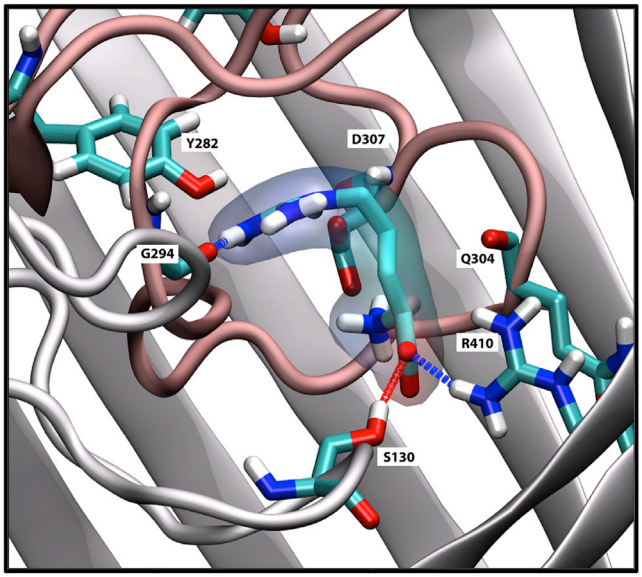

FIGURE 4 (*Close-up snapshot*) An arginine substrate, with the backbone carboxylate pointing toward the periplasmic space, in the eyelet region of OprD. (*Dashed lines*) Hydrogen bonds. To see this figure in color, go online.

PorB

PorB is a trimeric porin from *Neisseria meningitidis* that is instrumental in serious infections such as bacterial meningitis. As a porin, it is also one of the major entryways for antibiotic molecules into Gram-negative bacteria. Experimentally, it is known that PorB exhibits relatively large conductance and selectivity for anions, although the molecular origin of the selectivity is not comprehensively understood. Pioneering MD simulations, in which two bilayers are employed to form two distinct compartments, allowed Kutzner et al. (62) to simulate ion flux through the PorB channel based on biologically realistic electrochemical gradients. The simulations revealed crucial mechanistic insights: namely, that anions almost exclusively pass along a cluster of basic residues on one side of the barrel, whereas cations move along acidic residues lining the opposite side. Thus, there is almost no overlap between the pathways taken by cations and anions through PorB. The advantages of the double-bilayer approach, which has been termed "computational electrophysiology", are that it is applicable to channels of varying conductance; it is implemented within the popular GROMACS simulation code; and in close analogy to single-channel electrophysiology, physiologically and experimentally relevant timescales are achieved.

Protein-protein interactions in the outer membrane

While the importance of protein crowding in biological membranes is now well established (63), simulation studies that address this issue are still fairly scarce. Goose and

Sansom (64) and Chavent et al. (65) have recently reported coarse-grained simulations of bacterial membranes, which incorporate multiple copy numbers of proteins. The effect of crowding on the lateral movement of several OMPs (FhuA, LamB, NanC, OmpA, and OmpF) was assessed. Increasing the protein concentration within the bilayer led to reduced diffusion coefficients for both lipid and protein components. Interestingly, the lipid diffusion was particularly reduced in the vicinity of the proteins, forming an annulus of lipids as far as 20–30 Å away from the protein. Formation of extended clusters and networks of proteins was also reported from these simulations. Recently, Chavent et al. (65) reported similar linear protein aggregates appearing after ~1 μs of simulation of coarse-grain models incorporating 256 copies of the protein OmpA embedded in a 120 $\times$ 120 nm bilayer composed of 3:1 mixture of POPE-POPG lipids (Fig. 5). Similar simulations of large outer membrane systems were also reported by Khalid et al. (66). These large systems create new issues in term of analysis and visualization to decipher the intricate interdependency of proteins and lipids. To address this, Chavent et al. (65) have defined new illustrative representations of membrane dynamics using streamline methodology inspired by analysis of transient flows in macroscopic systems such as oceans or the atmosphere.

Conclusions

The last decade has seen exciting advances in the scope of bacterial membrane simulation studies. Atomistic simulations of complex membranes have become possible with the advent of parameters for lipopolysaccharides and complex phospholipids such as lysyl-PG. Future directions in terms of adding biological complexity to bacterial models will include constructing models of the peptidoglycan, the sugar-peptide polymers that reside within the periplasmic space between the two membranes of Gram-negative bacteria. Given the complex mixture of lipids in these membrane models and the slow rates of diffusion of some of the larger molecules, methods to reduce the amount of manual intervention required in setting up simulations, such as those of the CHARMM-GUI Membrane Builder (67) and MEMBUILDER (68), will become invaluable. In addition, resources for sharing parameters for membrane protein simulations, as well as the trajectory data itself, are also becoming extremely useful tools for comparative and high throughput simulations (69–73).

At the coarse-grain level of resolution, advances have been in terms of size as well as complexity; larger, complex systems were simulated for extended timescales. With these models and methods it is now possible to study protein and lipid diffusion, and the interdependence of the protein-protein interactions and the effects of membrane curvature on these phenomena (64–66). Future work in this area will include adding coarse-grained models of the LPS component of the outer membrane, and extending the system sizes such that life-size models of outer membrane vesicles can be studied. In conclusion, given we are already well on the way to approaching experimental length and timescales with in silico methods, the future for bacterial membrane simulations holds enormous promise.

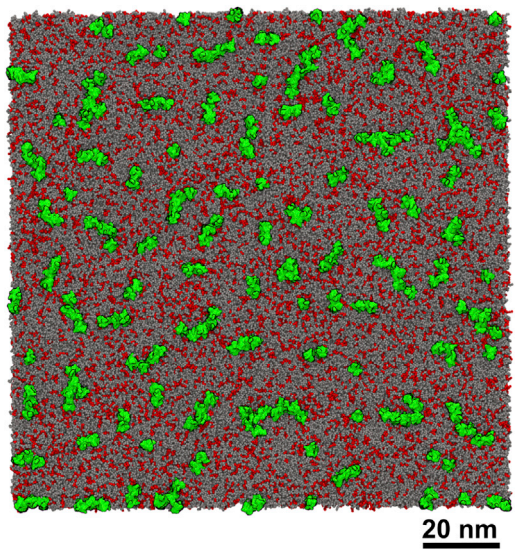

FIGURE 5 Porins clustering at the surface of a phospholipid membrane at the end of 1 μs of coarse-grain simulation. This simulation system is comprised of 256 copies of the *E. coli* protein OmpA embedded in a large bilayer (120 $\times$ 120 nm) composed of a 1:3 ratio of POPE and POPG phospholipids (65). To see this figure in color, go online.

ACKNOWLEDGMENTS

The authors thank Mark Sansom and Prapasiri Pongprayoon for providing the data for Fig. 3.

REFERENCES

1. Lugtenberg, E. J. J., and R. Peters. 1976. Distribution of lipids in cytoplasmic and outer membranes of *Escherichia coli* K12. *Biochim. Biophys. Acta.* 441:38–47.
2. Haest, C. W., J. de Gier, …, L. L. van Deenen. 1972. Changes in permeability of *Staphylococcus aureus* and derived liposomes with varying lipid composition. *Biochim. Biophys. Acta.* 255:720–733.
3. Cox, K., P. J. Bond, …, M. S. Sansom. 2008. Outer membrane proteins: comparing x-ray and NMR structures by MD simulations in lipid bilayers. *Eur. Biophys. J.* 37:131–141.
4. Bond, P. J., and M. S. Sansom. 2003. Membrane protein dynamics versus environment: simulations of OmpA in a micelle and in a bilayer. *J. Mol. Biol.* 329:1035–1053.
5. Denning, E. J., and O. Beckstein. 2013. Influence of lipids on protein-mediated transmembrane transport. *Chem. Phys. Lipids.* 169:57–71.
6. Vanegas, J. M., and M. Arroyo. 2014. Force transduction and lipid binding in MscL: a continuum-molecular approach. *PLoS One.* 9:e113947.
7. Weise, C. F., F. H. Login, …, M. Wolf-Watz. 2014. Negatively charged lipid membranes promote a disorder-order transition in the *Yersinia* YscU protein. *Biophys. J.* 107:1950–1961.

8. Wu, E. L., P. J. Fleming, …, W. Im. 2014. *E. coli* outer membrane and interactions with OmpLA. *Biophys. J.* 106:2493–2502.
9. Myung, H. J., R. Sakamaki, …, S. Lee. 2010. Accelerating molecular dynamics simulation using graphics processing unit. *Bull. Korean Chem. Soc.* 31:3639–3643.
10. Shaw, D. E., M. M. Deneroff, …, S. C. Wang. 2008. ANTON, a special-purpose machine for molecular dynamics simulation. *Commun. ACM.* 51:91–97.
11. Shaw, D. E., R. O. Dror, …, B. Towles. 2009. Millisecond-scale molecular dynamics simulations on ANTON. *In* Proceedings of the Conference on High Performance Computing Networking, Storage and Analysis, SC 2009, Portland, OR. Article No. 39. ACM, New York.
12. Noinaj, N., A. J. Kuszak, …, S. K. Buchanan. 2014. Lateral opening and exit pore formation are required for BamA function. *Structure.* 22:1055–1062.
13. G. A. Voth, editor 2008. Coarse-Graining of Condensed Phase and Biomolecular Systems. CRC Press, Boca Raton, FL.
14. Hong, C., D. P. Tieleman, and Y. Wang. 2014. Microsecond molecular dynamics simulations of lipid mixing. *Langmuir.* 30:11993–12001.
15. Lins, R. D., and T. P. Straatsma. 2001. Computer simulation of the rough lipopolysaccharide membrane of *Pseudomonas aeruginosa*. *Biophys. J.* 81:1037–1046.
16. Cornell, W. D., P. Cieplak, …, P. A. Coleman. 1996. A second generation force field for the simulation of proteins, nucleic acids, and organic molecules (vol 117, pg 5179, 1995). *J. Am. Chem. Soc.* 118:2309.
17. Woods, R. J., R. A. Dwek, …, B. Fraser-Reid. 1995. Molecular mechanical and molecular dynamical simulations of glycoproteins and oligosaccharides. 1. GLYCAM-93 parameter development. *J. Phys. Chem.* 99:3832–3846.
18. Piggot, T. J., D. A. Holdbrook, and S. Khalid. 2011. Electroporation of the *E. coli* and *S. aureus* membranes: molecular dynamics simulations of complex bacterial membranes. *J. Phys. Chem. B.* 115:13381–13388.
19. Oostenbrink, C., A. Villa, …, W. F. van Gunsteren. 2004. A biomolecular force field based on the free enthalpy of hydration and solvation: the GROMOS force-field parameter sets 53A5 and 53A6. *J. Comput. Chem.* 25:1656–1676.
20. Wu, E. L., O. Engström, …, W. Im. 2013. Molecular dynamics and NMR spectroscopy studies of *E. coli* lipopolysaccharide structure and dynamics. *Biophys. J.* 105:1444–1455.
21. Guvench, O., S. N. Greene, …, A. D. Mackerell, Jr. 2008. Additive empirical force field for hexopyranose monosaccharides. *J. Comput. Chem.* 29:2543–2564.
22. Guvench, O., E. R. Hatcher, …, A. D. Mackerell. 2009. CHARMM additive all-atom force field for glycosidic linkages between hexopyranoses. *J. Chem. Theory Comput.* 5:2353–2370.
23. Hatcher, E., O. Guvench, and A. D. Mackerell. 2009. CHARMM additive all-atom force field for aldopentofuranoses, methyl-aldopentofuranosides, and fructofuranose. *J. Phys. Chem. B.* 113:12466–12476.
24. Guvench, O., S. S. Mallajosyula, …, A. D. Mackerell, Jr. 2011. CHARMM additive all-atom force field for carbohydrate derivatives and its utility in polysaccharide and carbohydrate-protein modeling. *J. Chem. Theory Comput.* 7:3162–3180.
25. Pastor, R. W., and A. D. Mackerell, Jr. 2011. Development of the CHARMM force field for lipids. *J. Phys. Chem. Lett.* 2:1526–1532.
26. Mallajosyula, S. S., O. Guvench, …, A. D. Mackerell, Jr. 2012. CHARMM additive all-atom force field for phosphate and sulfate linked to carbohydrates. *J. Chem. Theory Comput.* 8:759–776.
27. Tarek, M. 2005. Membrane electroporation: a molecular dynamics simulation. *Biophys. J.* 88:4045–4053.
28. Tieleman, D. P. 2004. The molecular basis of electroporation. *BMC Biochem.* 5:10.
29. Song, J., C. Ji, and J. Z. Zhang. 2014. Insights on Na^+ binding and conformational dynamics in multidrug and toxic compound extrusion transporter NorM. *Proteins.* 82:240–249.
30. Vanni, S., P. Campomanes, …, U. Rothlisberger. 2012. Ion binding and internal hydration in the multidrug resistance secondary active transporter NorM investigated by molecular dynamics simulations. *Biochemistry.* 51:1281–1287.
31. Leung, Y. M., D. A. Holdbrook, …, S. Khalid. 2014. The NorM MATE transporter from *N. gonorrhoeae*: insights into drug and ion binding from atomistic molecular dynamics simulations. *Biophys. J.* 107: 460–468.
32. Seeger, M. A., A. Schiefner, …, K. M. Pos. 2006. Structural asymmetry of AcrB trimer suggests a peristaltic pump mechanism. *Science.* 313:1295–1298.
33. Touzé, T., J. Eswaran, …, V. Koronakis. 2004. Interactions underlying assembly of the Escherichia coli AcrAB-TolC multidrug efflux system. *Mol. Microbiol.* 53:697–706.
34. Masuda, N., E. Sakagawa, …, T. Nishino. 2000. Substrate specificities of MexAB-OprM, MexCD-OprJ, and MexXY-oprM efflux pumps in *Pseudomonas aeruginosa*. *Antimicrob. Agents Chemother.* 44:3322–3327.
35. Srikumar, R., E. Tsang, and K. Poole. 1999. Contribution of the MexAB-OprM multidrug efflux system to the β-lactam resistance of penicillin-binding protein and β-lactamase-derepressed mutants of *Pseudomonas aeruginosa*. *J. Antimicrob. Chemother.* 44:537–540.
36. Fischer, N., M. Raunest, …, C. Kandt. 2014. Efflux pump-mediated antibiotics resistance: insights from computational structural biology. *Interdiscip. Sci.* 6:1–12.
37. Fischer, N., and C. Kandt. 2011. Three ways in, one way out: water dynamics in the *trans*-membrane domains of the inner membrane translocase AcrB. *Proteins.* 79:2871–2885.
38. Schulz, R., A. V. Vargiu, …, P. Ruggerone. 2010. Functional rotation of the transporter AcrB: insights into drug extrusion from simulations. *PLOS Comput. Biol.* 6:e1000806.
39. Holdbrook, D. A., T. J. Piggot, …, S. Khalid. 2013. Stability and membrane interactions of an autotransport protein: MD simulations of the Hia translocator domain in a complex membrane environment. *Biochim. Biophys. Acta.* 1828:715–723.
40. Piggot, T. J., D. A. Holdbrook, and S. Khalid. 2013. Conformational dynamics and membrane interactions of the *E. coli* outer membrane protein FecA: a molecular dynamics simulation study. *Biochim. Biophys. Acta.* 1828:284–293.
41. Eren, E., J. Vijayaraghavan, …, B. van den Berg. 2012. Substrate specificity within a family of outer membrane carboxylate channels. *PLoS Biol.* 10:e1001242.
42. Tamber, S., M. M. Ochs, and R. E. Hancock. 2006. Role of the novel OprD family of porins in nutrient uptake in *Pseudomonas aeruginosa*. *J. Bacteriol.* 188:45–54.
43. Baslé, A., G. Rummel, …, T. Schirmer. 2006. Crystal structure of osmoporin OmpC from *E. coli* at 2.0 Å. *J. Mol. Biol.* 362:933–942.
44. Cowan, S. W., R. M. Garavito, …, T. Schirmer. 1995. The structure of OmpF porin in a tetragonal crystal form. *Structure.* 3:1041–1050.
45. Jaffe, A., Y. A. Chabbert, and O. Semonin. 1982. Role of porin proteins OmpF and OmpC in the permeation of β-lactams. *Antimicrob. Agents Chemother.* 22:942–948.
46. James, C. E., K. R. Mahendran, …, J. M. Pagès. 2009. How β-lactam antibiotics enter bacteria: a dialogue with the porins. *PLoS One.* 4:e5453.
47. Moraes, T. F., M. Bains, …, N. C. Strynadka. 2007. An arginine ladder in OprP mediates phosphate-specific transfer across the outer membrane. *Nat. Struct. Mol. Biol.* 14:85–87.
48. Pongprayoon, P., O. Beckstein, …, M. S. Sansom. 2009. Simulations of anion transport through OprP reveal the molecular basis for high affinity and selectivity for phosphate. *Proc. Natl. Acad. Sci. USA.* 106:21614–21618.
49. Sukhan, A., and R. E. W. Hancock. 1996. The role of specific lysine residues in the passage of anions through the *Pseudomonas aeruginosa* porin OprP. *J. Biol. Chem.* 271:21239–21242.

50. Modi, N., I. Bárcena-Uribarri, …, U. Kleinekathöfer. 2014. Tuning the affinity of anion binding sites in porin channels with negatively charged residues: molecular details for OprP. *ACS Chem. Biol.*

51. Modi, N., I. Bárcena-Uribarri, …, U. Kleinekathöfer. 2013. Role of the central arginine R133 toward the ion selectivity of the phosphate specific channel OprP: effects of charge and solvation. *Biochemistry.* 52:5522–5532.

52. Biswas, S., M. M. Mohammad, …, B. van den Berg. 2007. Structural insight into OprD substrate specificity. *Nat. Struct. Mol. Biol.* 14:1108–1109.

53. Eren, E., J. Parkin, …, B. van den Berg. 2013. Toward understanding the outer membrane uptake of small molecules by *Pseudomonas aeruginosa*. *J. Biol. Chem.* 288:12042–12053.

54. Parkin, J., and S. Khalid. 2014. Atomistic molecular-dynamics simulations enable prediction of the arginine permeation pathway through OccD1/OprD from *Pseudomonas aeruginosa*. *Biophys. J.* 107:1853–1861.

55. Kumar, A., E. Hajjar, …, M. Ceccarelli. 2010. Molecular simulations reveal the mechanism and the determinants for ampicillin translocation through OmpF. *J. Phys. Chem. B.* 114:9608–9616.

56. Singh, P. R., M. Ceccarelli, …, K. R. Mahendran. 2012. Antibiotic permeation across the OmpF channel: modulation of the affinity site in the presence of magnesium. *J. Phys. Chem. B.* 116:4433–4438.

57. Kumar, A., E. Hajjar, …, M. Ceccarelli. 2010. Structural and dynamical properties of the porins OmpF and OmpC: insights from molecular simulations. *J. Phys. Condens. Matter.* 22:454125.

58. Stansfeld, P. J., and M. S. P. Sansom. 2011. Molecular simulation approaches to membrane proteins. *Structure.* 19:1562–1572.

59. Gumbart, J., Y. Wang, …, K. Schulten. 2005. Molecular dynamics simulations of proteins in lipid bilayers. *Curr. Opin. Struct. Biol.* 15:423–431.

60. Bond, P. J., and M. S. P. Sansom. 2004. The simulation approach to bacterial outer membrane proteins [Review]. *Mol. Membr. Biol.* 21:151–161.

61. Ash, W. L., M. R. Zlomislic, …, D. P. Tieleman. 2004. Computer simulations of membrane proteins. *Biochim. Biophys. Acta.* 1666:158–189.

62. Kutzner, C., H. Grubmüller, …, U. Zachariae. 2011. Computational electrophysiology: the molecular dynamics of ion channel permeation and selectivity in atomistic detail. *Biophys. J.* 101:809–817.

63. Jarosławski, S., K. Duquesne, …, S. Scheuring. 2009. High-resolution architecture of the outer membrane of the Gram-negative bacteria *Roseobacter denitrificans*. *Mol. Microbiol.* 74:1211–1222.

64. Goose, J. E., and M. S. P. Sansom. 2013. Reduced lateral mobility of lipids and proteins in crowded membranes. *PLOS Comput. Biol.* 9:e1003033.

65. Chavent, M., T. Reddy, …, M. S. Sansom. 2014. Methodologies for the analysis of instantaneous lipid diffusion in MD simulations of large membrane systems. *Faraday Discuss.* 169:455–475.

66. Khalid, S., N. A. Berglund, …, J. Parkin. 2015. The membranes of Gram-negative bacteria: progress in molecular modelling and simulation. *Biochem. Soc. Trans.* 43:162–167.

67. Wu, E. L., X. Cheng, …, W. Im. 2014. CHARMM-GUI Membrane Builder: toward realistic biological membrane simulations. *J. Comput. Chem.* 35:1997–2004.

68. Ghahremanpour, M. M., S. S. Arab, …, D. van der Spoel. 2014. MEMBUILDER: a web-based graphical interface to build heterogeneously mixed membrane bilayers for the GROMACS biomolecular simulation program. *Bioinformatics.* 30:439–441.

69. Sansom, M. S., K. A. Scott, and P. J. Bond. 2008. Coarse-grained simulation: a high-throughput computational approach to membrane proteins. *Biochem. Soc. Trans.* 36:27–32.

70. Tsirigos, K. D., P. G. Bagos, and S. J. Hamodrakas. 2011. OMPdb: a database of β-barrel outer membrane proteins from Gram-negative bacteria. *Nucleic Acids Res.* 39:D324–D331.

71. Domański, J., P. J. Stansfeld, …, O. Beckstein. 2010. Lipidbook: a public repository for force-field parameters used in membrane simulations. *J. Membr. Biol.* 236:255–258.

72. Stansfeld, P. J., J. E. Goose, …, M. Sansom. 2015. MemProtMD: automated insertion of membrane protein structures into explicit lipid membranes. *Structure.* 23:1350–1361.

73. Raman, P., V. Cherezov, and M. Caffrey. 2006. The Membrane Protein Data Bank. *Cell. Mol. Life Sci.* 63:36–51.